

A. Rabhi,<sup>1,\*</sup> P. Schuck,<sup>2,3,†</sup> and J. Da Providência<sup>1,‡</sup>

<sup>1</sup>*Departamento de Física, Universidade de Coimbra, 3004-516 Coimbra, Portugal*

<sup>2</sup>*Institut de Physique Nucléaire, 91406 Orsay Cedex, France*

<sup>3</sup>*LPM2C, Maison des Magistères-CNRS, 25, avenue des Martyrs, BP 166, 38042, Grenoble Cedex, France*

(Dated: September 11, 2018)

The Hartree-Fock-RPA approach is applied to the 1D anti-ferromagnetic Heisenberg model in the Jordan-Wigner representation. Somewhat contrary to expectation, this leads to reasonable results for spectral functions and sum rules in the symmetry unbroken phase.

PACS numbers: 75.40.Gb, 75.50.Ee, 75.10.Pq

The 1D Anti-Ferromagnetic Heisenberg Model (AFHM)<sup>1</sup> belongs to one of the most classic many body research fields. It has been the first many-body model to be solved exactly by Bethe with his famous Bethe ansatz solution<sup>2</sup> and it has been a playground for testing and developing many body approaches ever since. In spite of tremendous progress in the understanding of many facets of the model, it continues to be a very active field of interest and research<sup>3</sup>.

In an attempt to apply extended RPA-like theories, as *e.g.* the recently developed Self-Consistent RPA (SCRPA) approach<sup>5,6</sup>, we found out, somewhat to our surprise, that even the standard RPA theory has so far not fully been developed in its application to the 1D-AFHM. This probably stems from the fact that the HF-RPA scheme is usually considered as unreliable in low dimensions<sup>7</sup>. However, it will be found that RPA shows interesting features even in this 1D-version of the model.

We mostly consider the isotropic Heisenberg model with anti-ferromagnetic coupling, however some consideration will also be given to the anisotropic case, for instance to the XXZ-anisotropic Heisenberg Hamiltonian

$$H = \sum_{n=1}^N \left\{ \frac{1}{2} (S_{n+1}^+ S_n^- + S_{n+1}^- S_n^+) + g S_{n+1}^z S_n^z \right\}. \quad (1)$$

where  $S_n^i$  is the spin operator of the  $n$ -th site,  $g$  is the anisotropy parameter and  $N$  is the number of sites. Periodic boundary conditions ( $S_{N+1}^i = S_1^i$ ) are applied. We will work with the AFH model in the Jordan-Wigner (JW) representation<sup>8</sup>. The Hamiltonian in momentum representation is given by<sup>9</sup>

$$H = \frac{gN}{4} + \sum_k \varepsilon_k^o \psi_k^\dagger \psi_k + \frac{1}{4} \sum_{k_1 k_2 k_3 k_4} \bar{v}_{k_1 k_2 k_3 k_4} \psi_{k_1}^\dagger \psi_{k_2}^\dagger \psi_{k_4} \psi_{k_3} \quad (2)$$

with

$$\varepsilon_p^o = \cos(k) - g \quad (3)$$

and

$$\bar{v}_{k_1 k_2 k_3 k_4} = \frac{2g}{N} (\cos(k_1 - k_3) - \cos(k_1 - k_4)) \delta(k_1 + k_2 - k_3 - k_4). \quad (4)$$

The isotropic point is given by  $g = 1$  whereas for  $g \neq 1$  we have the XXZ model. In order to take care of the boundary conditions the momentum sums run over the values  $k = j \frac{\pi}{N}$  with :

$$\begin{aligned} j &= \pm 1, \pm 3, \pm 5, \dots, \pm(N-1) && \text{for } n \text{ even} \\ j &= 0, \pm 2, \pm 4, \dots, \pm(N-2), N && \text{for } n \text{ odd} \end{aligned} \quad (5)$$

where  $n$  is the fermion number (in this note we only consider the sector  $n = N/2$ ) and where we have assumed, without loss of generality, that  $N$  is even. The Kronecker symbol is defined by :

$$\begin{aligned} \delta(p - p') &= 1 && \text{if } p = p' \pm 2\pi\tau; \quad \tau = 0, 1, 2, \dots \\ &= 0 && \text{otherwise.} \end{aligned} \quad (6)$$

We first want to study the Hartree-Fock (HF) approximation, keeping translational invariance, *i.e.* momentum as a good quantum number. The JW-HF single particle energies are given by  $\epsilon_k = \langle \{ \psi_k, [H, \psi_k^\dagger] \} \rangle$ . Here  $[.., ..]$  stands

for commutator,  $\{...,...\}$  for anticommutator, and  $\langle...\rangle$  denotes the expectation value in the HF state. One obtains

$$\epsilon_k = \epsilon_k^o + \frac{2g}{N} \sum_h (1 - \cos(k-h)). \quad (7)$$

where the sum goes over the occupied states "h" only. The HF groundstate energy is then given by

$$E_0^{HF} = \frac{gN}{4} + \sum_h \left( \epsilon_h^o + \frac{g}{N} \sum_{h'} (1 - \cos(h-h')) \right). \quad (8)$$

It is interesting to note that with respect to the Néel state the HF energy of the JW transformed isotropic AF Hamiltonian has actually a lower minimum. In table I we give the HF energy for the Néel state and the JW-HF energies as a function of the number of sites  $N$  for the isotropic situation with  $g = 1$ . So the JW-HF theory takes

N	4	6	8	12
Néel energy	-1.0	-1.5	-2.0	-3.0
JW-HF energy	-1.9142	-2.6667	-3.4667	-5.1077
Deformed JW-HF energy	-1.9142	-2.6667	-3.4856	-5.1927

TABLE I: Mean-field energies with various sophistications for some low number of site cases (see text for details).

into account more of the interaction energy than the Néel state in real space. It seems, however, not easy to analyze the physical content in real space of the JW-HF groundstate. For illustration we also show in Fig. 1 the JW-HF groundstate energy as a function of  $g$  for  $N = 6$  and compare with the exact solution.

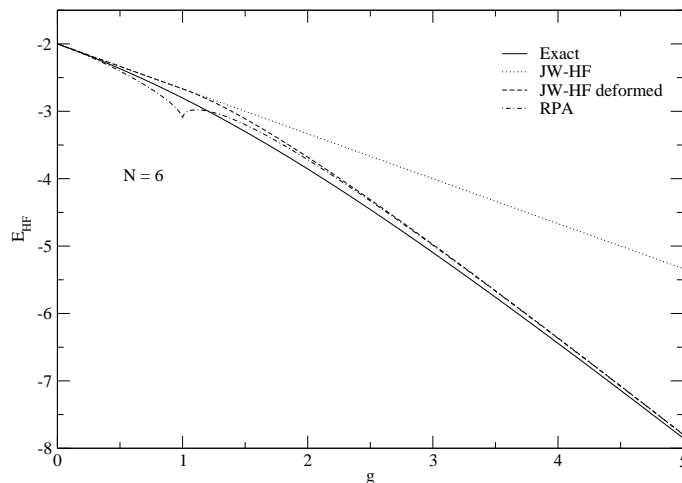


FIG. 1: Exact, RPA and HF groundstate energies in both spherical and deformed basis in the case of  $N = 6$ .

We now go one step further and investigate the Random Phase Approximation to describe excitations on top of the before considered JW-HF groundstate. For this we elaborate the RPA equations via the equation of motion (EOM) method<sup>10,11</sup>. We introduce an RPA particle(p)-hole(h) excitation operator

$$Q_\nu^\dagger = \sum_{ph} X_{ph}^\nu \psi_p^\dagger \psi_h - Y_{ph}^\nu \psi_h^\dagger \psi_p \quad (9)$$

with  $|\nu\rangle = Q_\nu^\dagger|0\rangle$  and  $|\nu\rangle, |0\rangle$  the excited state and groundstate respectively. With the vacuum condition  $Q_\nu|0\rangle = 0$  and approximating  $|0\rangle$  by the HF state one arrives as usual<sup>12</sup> to the RPA eigenvalue equation

$$\sum_{p'h'} \begin{pmatrix} A & B \\ -B^* & -A^* \end{pmatrix}_{ph,p'h'} \begin{pmatrix} X_{p'h'}^\nu \\ Y_{p'h'}^\nu \end{pmatrix} = \Omega_\nu \begin{pmatrix} X_{p'h'}^\nu \\ Y_{p'h'}^\nu \end{pmatrix} \quad (10)$$

with

$$\begin{aligned} A_{ph,p'h'} &= \langle [\psi_h^\dagger \psi_p, [H, \psi_{p'}^\dagger \psi_{h'}]] \rangle \\ &= (\epsilon_p - \epsilon_h) \delta_{pp'} \delta_{hh'} + \bar{v}_{ph',hp'} \end{aligned} \quad (11a)$$

$$B_{ph,p'h'} = -\langle [\psi_h^\dagger \psi_p, [H, \psi_{h'}^\dagger \psi_{p'}]] \rangle = \bar{v}_{pp',hh'} \quad (11b)$$

We get the standard RPA from Eqs.(10) in evaluating expectation values with the before elaborated JW-HF ground-state leading to the expressions given in Eq.(11). We show in Fig. 2 for  $N = 180$  and  $g = 1$  the RPA eigenvalue spectrum as a function of the momentum transfer  $|q|$ . We clearly see that there is a lower branch slightly detached

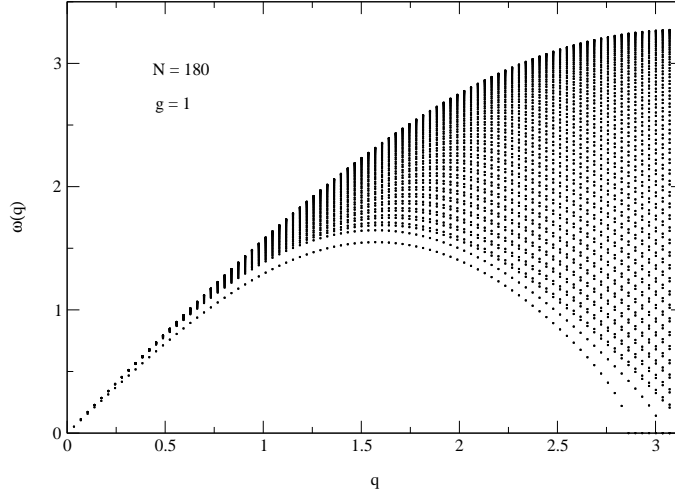


FIG. 2: RPA Excitation spectrum for  $N = 180$  and  $g = 1$ .

from the more or less dense remainder *i.e.* the p-h continuum. Actually  $N = 180$  is already quite close to the thermodynamic limit which we also calculated using the Green function method following closely the work of Todani and Kawasaki<sup>13</sup>. We will give details of this development in a forthcoming paper. Here we only show the result in Fig. 3. We again see that a lower energy state (lowest broken line) becomes detached from the continuum, the latter being embraced by the two upper broken lines. The continuum was also studied by Todani and Kawasaki<sup>13</sup> but for some reason they did not discuss the low-lying discrete state which is an important and prominent feature. In the thermodynamic limit the dispersion equation of the low-lying branch can be found from (see Ref.<sup>13</sup> Eq.(34))

$$1 - \Sigma(q, \omega) \Re(G^0(q, \omega)) = 0 \quad (12)$$

where  $G^0(q, \omega)$  is the renormalized particle-hole propagator<sup>13</sup>

$$G^0(q, \omega) = \frac{-1}{p\pi \sin(\frac{q}{2})} \frac{1}{2\sqrt{1-x^2}} \log \left( \frac{\sqrt{1-x^2} + \sin(\frac{q}{2})}{\sqrt{1-x^2} - \sin(\frac{q}{2})} \right), \quad (13)$$

and

$$\Sigma(q, \omega) = 2 \cos(q) - 2px^2 \quad (14)$$

with  $x = \frac{\omega + i\eta}{2p \sin(\frac{q}{2})}$  and  $p = 1 + \frac{2}{\pi}$ . From Eq. (12) also the lower  $\omega_L$  and upper  $\omega_U$  boundaries of the continuum can be obtained

$$\omega_L = \left(1 + \frac{2}{\pi}\right) \sin(q) \quad (15a)$$

$$\omega_U = 2\left(1 + \frac{2}{\pi}\right) \sin\left(\frac{q}{2}\right). \quad (15b)$$

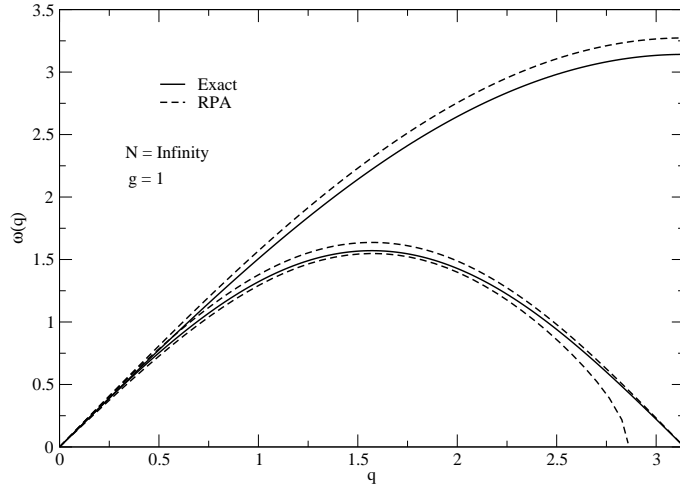


FIG. 3: Excitation spectrum for the infinite chain. The lowest broken line corresponds to the discrete RPA branch. The two upper broken lines limit the RPA p-h continuum. The two full lines limit the continuum in the exact two-spinon case<sup>4</sup> where there is no discrete state.

In the exact two-spinon case there is no discrete state and only a continuum limited by the upper ( $\omega_U = \pi \sin(\frac{q}{2})$ ) and lower ( $\omega_L = \frac{\pi}{2} \sin(q)$ ) full lines of Fig. 3 exists<sup>4,14</sup>. The exact two-spinon spectrum diverges at the lower limit<sup>4,14</sup>. Nevertheless, globally, the RPA spectrum for the infinite chain resembles the exact solution, even though locally, especially at the lower edge, things go wrong even qualitatively. For instance, the fact that the excitation spectrum exhibits a low lying discrete state detached from the continuum is of course an artefact of the RPA approach. Besides that, however, the RPA spectrum is already qualitatively similar to the exact one as seen in Fig. 4 where we show the structure functions for  $q = \frac{\pi}{2}$  and  $q = \frac{3\pi}{4}$  corresponding to RPA and exact two-spinon calculation<sup>4</sup>. We also can compare the following energy weighted sum rules

$$\frac{1}{2\pi} \int_0^\infty \omega S_{zz}(q, \omega) d\omega = -\frac{2E_{gs}}{3N}(1 - \cos(q)) \quad (16a)$$

$$\frac{1}{2\pi} \int_0^\infty \omega S_{zz}^{(2)}(q, \omega) d\omega = \frac{C}{\pi} \kappa_0 (1 - \cos(q)) \quad (16b)$$

$$\frac{1}{2\pi} \int_0^\infty \omega S_{zz}^{RPA}(q, \omega) d\omega = \frac{1}{\pi} (1 - \cos(q)) \quad (16c)$$

with  $C = 0.72221\dots$ ,  $\kappa_0 = 0.9163\dots$  and  $E_{gs} = -N(\log 2 - \frac{1}{4})$  being the exact ground-state energy.  $S_{zz}(q, \omega)$  is the exact dynamic spin structure factor,  $S_{zz}^{(2)}(q, \omega)$  is the exact 2-spinon part of the exact dynamic spin structure factor<sup>4</sup>, and  $S_{zz}^{RPA}(q, \omega)$  is the corresponding structure function in the present RPA approach. For  $q = \frac{\pi}{2}$ , in RPA, the sum rule gives 0.31830989 and the contribution to the sum rule from the discrete state is 0.226843 (71%) and from the continuum it is 0.09146731 (29%). For  $q = \frac{3\pi}{4}$ , in RPA, the sum rule gives 0.54338897 and the contribution to the sum rule from the discrete state is 0.244919 (45%) and from the continuum it is 0.29846996 (55%). From the above we see that the RPA energy weighted sum rule is within  $\sim 8\%$  of the exact result and within  $\sim 50\%$  of the exact two-spinon result.

To the best of our knowledge we are not aware of any earlier discussion of the existence of the low-lying discrete state in RPA. As already mentioned, only the continuum part of the spectral function in Fig. 4 has been discussed by Todani and Kawasaki<sup>13</sup> in the  $N \rightarrow \infty$  limit.

This overlooked discrete state is probably also the reason why it has not been noticed that the RPA as treated here is actually built on an unstable HF-groundstate. This is seen from the discrete lower branch in Fig. 2 and Fig. 3, touching zero at about  $q = q_c = 0.91\pi$ . An RPA eigenvalue coming down to zero inevitably means that the

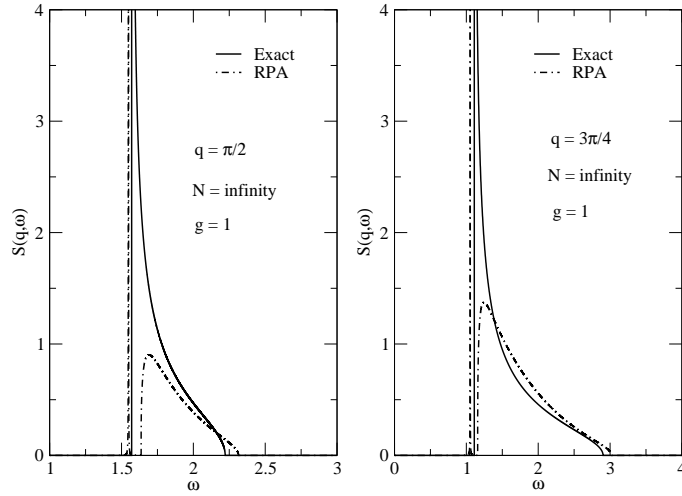


FIG. 4: Exact two-spinon and RPA dynamic spin structure factor, in the thermodynamic limit, for  $q = \frac{\pi}{2}$  and  $q = \frac{3\pi}{4}$ .

corresponding HF stability matrix<sup>11</sup>

$$\mathcal{S}(q) = \begin{pmatrix} A & B \\ B & A \end{pmatrix} \quad (17)$$

also has a zero eigenvalue at the critical value  $q = q_c$  and negative eigenvalues for  $q > q_c$ , clearly indicating that the translationally invariant JW-HF solution is unstable.

This feature is best illustrated in Fig. 5 where we show the low-lying part of the RPA spectrum for  $N = 6$  as a function of  $g$ . We see that the lowest detached eigenvalue for  $q = \pi$  touches ground at  $g = g_c = 1$ . We can check that for  $N = 4$   $g_c = \sqrt{2}$ , and for  $N = 180$   $g_c = 0.32$ . We will show below that for  $N \rightarrow \infty$   $g_c \rightarrow 0$ . Therefore the spectra shown in Figs. 2,3,4 correspond to situation already deep in the unstable region. The reason why the RPA performs relatively well is probably precisely because we forced the system to remain in the symmetry unbroken, i.e. 'spherical', phase as it is well known that in 1D no spontaneously symmetry broken phase exists. None the less, we were curious to see what HF and HF-RPA gives in the symmetry broken phase. Not unexpectedly we will find that deformed HF still lowers the energy (see table I) but HF-RPA leads to an unphysical excitation spectrum. Follow some details of our procedure.

We seek a new HF basis with a stable minimum in introducing new quasiparticles operators which are a superposition of particle (p) and hole (h) operators in the old basis, that is<sup>15</sup>

$$\begin{aligned} \alpha_{h+\pi}^\dagger &= u_h \psi_{h+\pi}^\dagger + v_h \psi_h^\dagger \\ \alpha_h &= u_h \psi_h^\dagger - v_h \psi_{h+\pi}^\dagger \end{aligned} \quad (18)$$

with  $u_h^2 + v_h^2 = 1$ . Our ansatz Eq.(18) is motivated by the fact that the mode which becomes unstable occurs at  $q = \pi$  and therefore, suggests the order parameter  $\langle \psi_{h+\pi}^\dagger \psi_h \rangle \neq 0$ , ensuing breaking of translational invariance. Following the standard procedure for obtaining the amplitudes  $u_h, v_h$  in Eq.(18) we express the HF-energy in the new deformed state

$$\begin{aligned} \tilde{E}_0^{HF} &= \frac{gN}{4} + \sum_h \left( \epsilon_h^o + \frac{1}{2} \sum_{h'} \bar{v}_{h,h',h,h'} \right) \\ &+ \sum_h \left( \epsilon_{h+\pi}^o - \epsilon_h^o + \sum_{h'} \left\{ \bar{v}_{h+\pi,h',h+\pi,h'} - \bar{v}_{h,h',h,h'} \right. \right. \\ &\left. \left. + \frac{1}{2} (\bar{v}_{h+\pi,h'+\pi,h+\pi,h'+\pi} + \bar{v}_{h,h',h,h'} - 2\bar{v}_{h+\pi,h',h+\pi,h'}) v_{h'}^2 \right\} v_h^2 \right) \end{aligned}$$

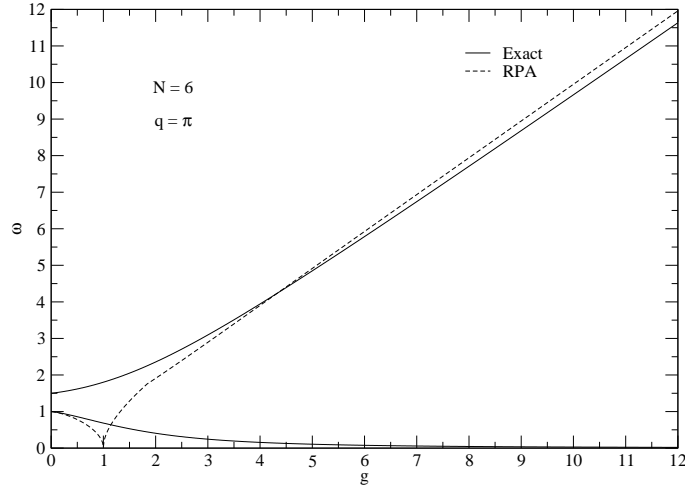


FIG. 5: Low-lying RPA mode as function of  $g$ , for  $N = 6$  (broken line) together with the exact solution (full line).

$$+ \sum_{hh'} (\bar{v}_{h+\pi, h'+\pi, h, h'} + \bar{v}_{h+\pi, h', h, h'+\pi}) u_h v_h u_{h'} v_{h'} \quad (19)$$

and minimize with respect to  $u_h, v_h$ . We obtain

$$\left. \begin{matrix} u_h^2 \\ v_h^2 \end{matrix} \right\} = \frac{1}{2} \left( 1 \pm \frac{\xi_h}{\sqrt{\xi_h^2 + \Delta_h^2}} \right) \quad (20)$$

where,

$$\begin{aligned} \xi_h &= \epsilon_{h+\pi}^o - \epsilon_h^o + \sum_{h' \neq h} \left\{ \left( \bar{v}_{h+\pi, h'+\pi, h+\pi, h'+\pi} + \bar{v}_{h, h', h, h'} \right. \right. \\ &\quad \left. \left. - \bar{v}_{h+\pi, h', h+\pi, h'} - \bar{v}_{h, h'+\pi, h, h'+\pi} \right) v_{h'}^2 \right. \\ &\quad \left. + \bar{v}_{h+\pi, h', h+\pi, h'} - \bar{v}_{h, h', h, h'} \right\} \\ \Delta_h &= -2 \sum_{h' \neq h} (\bar{v}_{h+\pi, h'+\pi, h, h'} - \bar{v}_{h+\pi, h', h'+\pi, h}) u_{h'} v_{h'} \end{aligned} \quad (21)$$

With Eq.(20) and Eq.(21) we get the self-consistent 'gap' equation

$$\Delta_h = -2 \sum_{h' \neq h} (\bar{v}_{h+\pi, h'+\pi, h, h'} - \bar{v}_{h+\pi, h', h'+\pi, h}) \frac{\Delta_{h'}}{2\sqrt{\xi_{h'}^2 + \Delta_{h'}^2}}. \quad (22)$$

Solving the gap equation numerically allows us to calculate the new HF energy as a function of  $g$ . For  $N \rightarrow \infty$  Eq. (22) gives a nontrivial solution even for  $g \rightarrow 0$ .

As a last step we calculate the RPA in the new basis. For this we introduce in analogy to Eq. (9) an RPA excitation operator of the following form

$$Q_{\nu, q}^\dagger = \sum_{ph} \tilde{X}_{ph}^\nu \alpha_p^\dagger \alpha_h^\dagger - \tilde{Y}_{ph}^\nu \alpha_h \alpha_p, \quad q = |p - h| \quad (23)$$

Proceeding in a similar way to what we have done in the spherical basis we can find the amplitudes  $\tilde{X}, \tilde{Y}$  from corresponding RPA equations. We show the spectrum in Fig. 6. We see that the spectrum now contains a gap

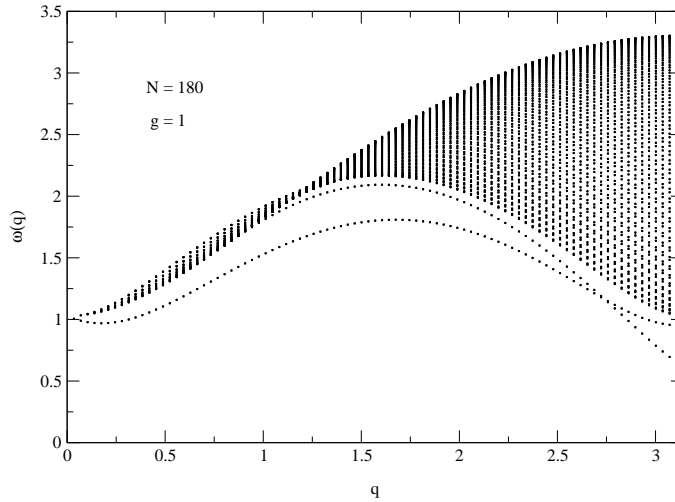


FIG. 6: RPA excitation spectrum in deformed basis in the case of  $N = 180$ .

corresponding to Eq. (21) and is qualitatively similar to the exact solutions for an anisotropic Heisenberg Hamiltonian ( $g \neq 1$ )<sup>3</sup>.

The fact that the spectrum in Fig. 6 does not resemble much the exact one is not completely surprising, since we know that it is built on qualitatively wrong (symmetry broken) groundstate. However, the relatively good performance of the HF-RPA scheme in the symmetry unbroken phase motivates us to go beyond the standard RPA approach in applying symmetry restoration techniques<sup>11</sup> and Self-Consistent RPA (SCRPA)<sup>5</sup>. The latter has already produced an interesting result for the 1D-AFHB model in Ref.<sup>6</sup>.

In summary, we evaluated for the first time the full RPA solution for the 1D Anti-Ferromagnetic Heisenberg model in the Jordan-Wigner representation. It is shown that one obtains interesting results for spectral functions and sum rules in the symmetry unbroken phase. The translationally invariant broken Hartree-Fock solution still lowers the energy but the corresponding RPA shows, not unexpectedly, an artificial gap in the spectrum.

### Acknowledgments

We thank H.-J. Mikeska, J. Vilain, T. Ziman for useful discussions and comments. One of us (A.R.) specially acknowledges many useful and elucidating discussions with C. Providência. This work has been supported by a grant provided by Fundação para a Ciência e a Tecnologia SFRH/BPD/14831/2003.

---

\* Electronic address: rabhi@teor.fis.uc.pt

† Electronic address: schuck@ipno.in2p3.fr

‡ Electronic address: providencia@teor.fis.uc.pt

<sup>1</sup> W. Heisenberg, Z. Phys. 49, 619 (1928).

<sup>2</sup> H. Bethe, Z. Phys. 71, 205 (1931).

<sup>3</sup> H.-J. Mikeska and A. K. Kolezhuk, Lecture Notes in Physics vol.645, p.1–83 (2004).

<sup>4</sup> A. H. Bougourzi, M. Couture and M. Kacir, Phys. Rev. B 54, R12669 (1996); M. Karbach, G. Müller, A. H. Bougourzi, A. Fledderjohann, and K.-H. Mütter, Phys. Rev. B 55, 12 510 (1997).

<sup>5</sup> J.G. Hirsch, A. Mariano, J. Dukelsky, P. Schuck, Ann. Phys. 296, 187 (2002); A. Rabhi, R. Bennaceur, G. Chanfray, and P. Schuck, Phys. Rev. C 66, 064315 (2002); A. Storozhenko, P. Schuck, J. Dukelsky, G. Röpke, A. Vdovin, Ann. Phys. 307, 308 (2003).

<sup>6</sup> P. Krüger and P. Schuck, EuroPhys. Lett. 72, 395 (1994).

<sup>7</sup> M. Takahashi, Phys. Rev. B 40, 2494 (1989).

<sup>8</sup> P. Jordan and E. Wigner, Z. Phys. 47, 631 (1928).

- <sup>9</sup> S. Rodriguez, Phys. Rev. 116, 14741477 (1959); E. Lieb, T. Schultz, and D. Maltis, Ann. Phys. (N.Y.) 16, 407 (1961); L. N. Bulaevski, Sov. Phys. JETP 16, 685 (1963).
- <sup>10</sup> D.J. Rowe, Phys. Rev. 175, 1283 (1968); Rev. Mod. Phys. 40, 153 (1968).
- <sup>11</sup> P. Ring and P. Schuck, *The Nuclear Many-Body Problem*, Springer, Berlin (1980)
- <sup>12</sup> D. J. Thouless, Nucl. Phys. 22, 78 (1961).
- <sup>13</sup> T. Todani and K. Kawasaki, Prog. Theor. Phys. 50, 1216 (1973).
- <sup>14</sup> G. Müller, H. Thomas, H. Beck, and J. C. Bonner, Phys. Rev. B 24, 1429 (1981).
- <sup>15</sup> A. Auerbach, *Interacting Electrons and Quantum Magnetism*, Springer-Verlag, New York (1994)